JOC The Journal of Organic Chemistry

Article

pubs.acs.org/joc

A Detailed NMR- and DFT-Based Study of the Sakurai–Hosomi–Yamamoto Asymmetric Allylation Reaction

David Hurem, Andrey G. Moiseev, Razvan Simionescu, and Travis Dudding*

Department of Chemistry, Brock University, 500 Glenridge Avenue, St. Catharines L2S 3A1, ON, Canada

Supporting Information

ABSTRACT: A Lewis acid complex between benzaldehyde and the silver catalyst was detected by ^{31}P NMR and shown to be the direct precursor to allylation within the Sakurai–Hosomi–Yamamoto reaction. Structural and thermochemical hybrid-DFT calculations indicated that benzaldehyde predominantly formed an η^1-σ-complex with the catalyst; however, two other competing conformers involving different coordination modes were found, including an activated μ^2-bound complex. The differences in ^{31}P NMR shifts upon complexation were calculated by the gauge-independent atomic orbital (GIAO–DFT) method for each conformer. The minimum energy conformer was found to correlate well with chemical shift trends observed experimentally, and an analysis of Mullikan charge populations revealed that the carbonyl carbon of the highest-energy conformer was the most electron-deficient. Furthermore, one minor and three major silicon intermediates were detected by ^{29}Si NMR and, with the aid of ^{1}H–^{29}Si HSQC, were assigned by comparison with parent compounds and GIAO–DFT calculations. Finally, a tentative mechanism was proposed based on these findings.

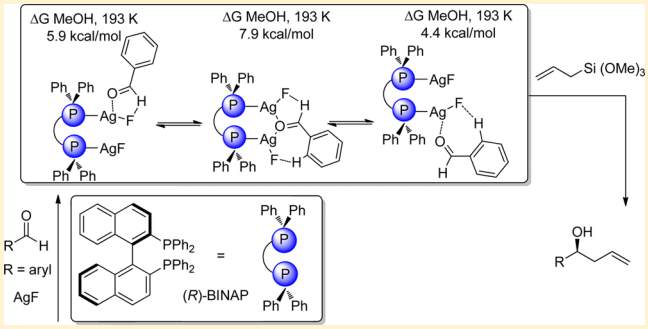

INTRODUCTION

Since the pioneering disclosure of the Lewis acid catalyzed C–C bond-forming addition of allylsilanes to carbonyls in 1976, the Sakurai reaction has become a mainstay in the field of synthesis for the construction of secondary and tertiary homoallylic alcohols [Scheme 1(a)].[1]

Scheme 1. Sakurai–Hosomi–Yamamoto Allylation

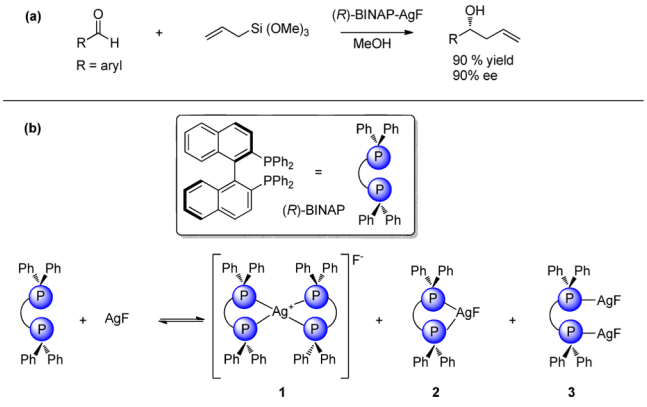

In line with these ideas, ongoing efforts toward the development of synthetic approaches to homoallylic alcohols continue to be driven by their recurrence in medicinal compounds, natural products, agrochemicals, and numerous other chemicals.[2] Consequently, as a part of these developments, the AgF-catalyzed Sakurai–Hosomi–Yamamoto allylation, reported by Yamamoto et al. in 1999, which employs (*R*)-(1,1′-binaphthalene-2,2′-diyl)bis(diphenylphosphine) [(*R*)-BINAP] as a chiral ligand, has emerged as a particularly important asymmetric transformation as it affords high levels of diastereo- and enantioselectivity and relies on the use of commercially available chiral ligands, aldehydes, and less toxic allylsilanes.[3] As for the mechanistic features of this reaction, it is noteworthy that Yamamoto and co-workers have provided the field with considerable mechanistic insight into and accompanying rationale for the Sakurai–Hosomi–Yamamoto allylation reaction and a number of other related Ag(I)-catalyzed processes.[3b,4] For instance, this group has reported a comprehensive ^{31}P NMR-, X-ray crystallographic data-, and UV–vis-supported mechanistic investigation of a (*R*)-BINAP$_2$·AgPF$_6$- and (*R*)-BINAP$_2$·AgOAc-catalyzed Mukaiyama aldol reaction that intriguingly afforded products of opposite absolute stereochemical configuration depending on which Ag(I) complex was used.[4] Certainly of greater relevance to the underlying mechanistic facets of the (*R*)-BINAP·AgF-catalyzed Sakurai–Hosomi–Yamamoto reaction have been ^{31}P NMR spectroscopic-based findings that revealed that the resting state of the catalyst in this reaction existed as a rapidly equilibrating temperature- and solvent-dependent mixture of Ag(I) species **2** and **3**, whereas the dominant species **1** formed irreversibly.[5]

Although the prior mechanistic studies addressing the (*R*)-BINAP·AgF-catalyzed Sakurai–Hosomi–Yamamoto reaction

Received: March 1, 2013
Published: April 9, 2013

   dx.doi.org/10.1021/jo400451u | J. Org. Chem. 2013, 78, 4440–4445

Table 1. ^{31}P NMR Data for the Catalytic Mixture with and without Benzaldehyde

	AgF/(*R*)-BINAP, 250 K[a]			AgF/(*R*)-BINAP benzaldehyde, 250 K[b]			AgF/(*R*)-BINAP benzaldehyde, 193 K[c]		
	J_{Ag-P}[d] (Hz)	integral (%)	δ_P (ppm)	J_{Ag-P} (Hz)	integral (%)	δ_P (ppm)	J_{Ag-P} (Hz)	integral (%)	δ_P (ppm)
1	242	6.6	16.3	242	7.3	16.3	242	6.4	17.1
2	405	18.9	13.9	389	20.3	14.0	402	19.1	14.7
3′ + **3**	–	–	–	682	72.4	2.1	–	–	–
3′	–	–	–	–	–	–	703	27.1	10.6
3	760	74.6	1.1	–	–	–	754	47.4	−1.6

[a]Spectra were obtained from (*R*)-BINAP (0.1 equiv) and AgF (0.06 equiv) in methanol-d_4 at 248.9 K. [b]Spectra were obtained in the presence of benzaldehyde (1.0 equiv) at 253.4 K. [c]Spectra were obtained in the presence of benzaldehyde (1.0 equiv) at 192.9 K. [d]Taken as an average between ^{107}Ag−P and ^{109}Ag−P coupling constants.

have provided insight into the resting state of the catalytic Ag(I) complexes involved in this transformation, still lacking at this time is a lucid mechanistic understanding of the Ag(I) species generated from the trimethoxysilane and aldehyde reagents used in this reaction. Importantly, this information would provide valuable insight into the transient catalytic species that serve as the direct progenitors to the high enantioselection of this process. The conventional wisdom regarding the mechanism of the Sakurai−Hosomi−Yamamoto allylation holds that three major Ag(I) complexes are formed under the reaction conditions that conform to (**1**) a dimeric (*R*)-BINAP$_2$·AgF complex that catalyzes a nonstereoselective background allylation; (**2**) a (*R*)-BINAP·AgF complex that has been thought to mediate an asymmetric (Type II) allylation via the transient interplay of a metal-based η^1-allyl intermediate, such as (*R*)-BINAP$_2$·Ag(CH$_2$CHCH$_2$); and (**3**) a (*R*)-BINAP·(AgF)$_2$ complex that induces enantioselection by way of a Lewis acid promoted (Type I) allylation process [Scheme 1(b)].[6] As such, working within the framework of ^{1}H, ^{13}C, and ^{31}P NMR spectroscopic studies and high-level DFT calculations, we report herein a mechanistic study of the Sakurai−Hosomi−Yamamoto reaction.

RESULTS AND DISCUSSION

At the outset of this study, we investigated the specific catalytic roles and structural nature of these entities through an analysis of the ^{31}P NMR spectra and J_{Ag-P} (that is, ^{31}P, ^{109}Ag, and ^{107}Ag) coupling constants of a mixture of AgF (10 equiv) and (*R*)-BINAP (6 equiv) cooled to the routinely used reaction temperature of 248.9 K (−24.1 °C). More specifically, it was apparent from this analysis that three distinct coordination complexes were present in the catalytic mixture in a ratio of 6:19:75, which were assigned as **1** (d, 16 ppm), **2** (d, 14 ppm), and **3** (d, 1 ppm), based upon the observed chemical shifts, average Ag−P spin−spin coupling constants (*J* value),[7] and the previous findings of Yamamoto et al. [Table 1 and Figure 1(a)].[5]

An excess of benzaldehyde (10 equiv) was then added to the sample under study at 253.4 K to gauge the extent to which the aldehyde component of this reaction interacted with the resting state(s) of the catalyst(s). The result was the noticeable broadening of the ^{31}P signal of the (*R*)-BINAP·(AgF)$_2$ complex (**3**) at 1 ppm into a poorly resolved doublet spanning the spectral region from 0 to 8 ppm (**3** + **3′**). In contrast, the signals assigned to **1** and **2** effectively remained unchanged [Figure 1(b)]. Aware of the dynamic nature of this catalytic system, we then probed the temperature dependence of this mixture by cooling the sample to 192.9 K (−80.1 °C), whereupon the broad signal spanning the spectral region from

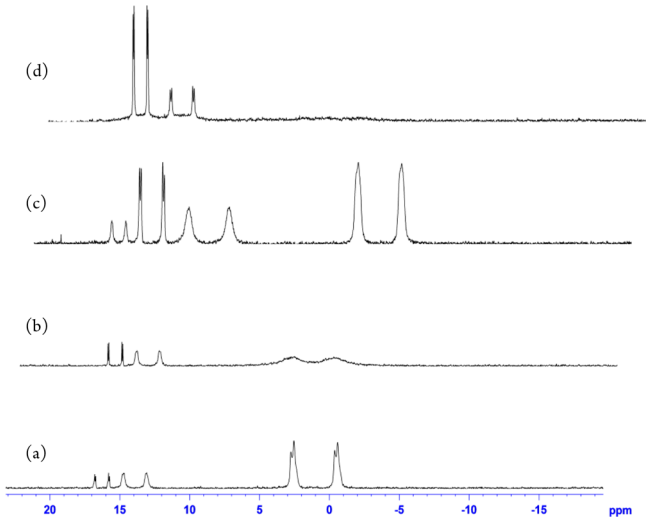

Figure 1. ^{31}P NMR spectra of (*R*)-BINAP (0.06 equiv) and AgF (0.1 equiv) (a) in methanol-d_4 at 248.9 K, (b) in the presence of benzaldehyde (1.0 equiv) at 253.4 K, (c) in the presence of benzaldehyde (1.0 equiv) at 192.9 K, and (d) in the presence of benzaldehyde (1.0 equiv) and allyltrimethoxysilane (1.5 equiv) at 233.8 K.

0 to 8 ppm sharpened into a well-resolved pair of doublets [Figure 1(c)]. The upfield doublet of this set at −1.56 ppm (J_{Ag-P} = 756 Hz) was assigned as the unbound complex **3**, whereas the lower field doublet (**3′**) at 10.6 ppm (d, J_{Ag-P} = 705 Hz) was thought to result from formation of a weighted distribution of aldehyde-bound complexes [(*R*)-BINAP·(AgF)$_2$*(O=C(H)Ph)$_n$ (*n* = 1 or 2)]. Consistent with this last assignment, the integrated area of the doublet at 10.6 ppm was equivalent in magnitude to that of the (*R*)-BINAP·(AgF)$_2$ complex present before the addition of benzaldehyde depicted in Figure 1(a) and Table 1.

Having found a temperature at which the signals assigned to **3** and **3′** were clearly resolved and to better understand the kinetic profile and respective off-and-on exchange rate of aldehyde and catalyst association, we progressively heated the sample of interest from 193 to ∼250 K (−20 °C). It was apparent from this analysis that the ^{31}P NMR signals assigned to **3** and **3′** coalesced at a temperature of ∼220 K (T_c) with a respective exchange frequency (k_r) of 3.2 × 10^3 s^{-1}, where $\Delta\nu$ is the full width of the peak at half of its maximum height at T_c (eq 1). From there, application of the Eyring equation results in a computed activation energy ($\Delta G^{\ddagger}$) of ∼7.2 kcal/mol for the formation of **3′** (eq 2).[8]

$$k_r = 2.2\Delta\nu \quad (1)$$

dx.doi.org/10.1021/jo400451u | J. Org. Chem. 2013, 78, 4440−4445

$$\Delta G^{\ddagger} = RT_c \ln\left(\frac{k_r h}{kT_c}\right) \quad (2)$$

Consistent with a host−guest-type interaction between benzaldehyde and the catalytic complex was the observation of an upfield singlet in both the acquired ^{1}H and ^{13}C spectra (5.57 and 97.2 ppm, respectively) at 193 K upon the addition of benzaldehyde. On the basis of $^{13}C-^{1}H$ HSQC data, these signals were found to be directly correlated and so were thought to correspond to the aldehyde hydrogen and carbon of benzaldehyde in the silver complex (see Supporting Information).

Despite strong support for benzaldehyde coordination, the type of complexation between benzaldehyde and the catalyst (**3**) was still not fully understood. It is well-known that the majority of main group, early transition metal, and lanthanide Lewis acids form σ-type complexes with carbonyl-containing compounds,[9a−c] while electron-rich transition metals form π-type complexes.[9a,d,e] Furthermore, σ-type complexation of aldehydes with Lewis acids has been shown to produce a downfield shift of ^{1}H and ^{13}C signals of the carbonyl group,[9c] and π-type complexes resonated upfield in comparison with the noncoordinated aldehyde.[9d,e] In this case, however, the presence of the sterically encumbering (*R*)-BINAP ligand makes it difficult to envision this reaction proceeding through a π-complex. On the other hand, it could be argued that a strong shielding effect induced by the aromatic system of the ligand could very well account for the observed upfield shift of ^{1}H and ^{13}C signals of benzaldehyde in the **3′** complex due to anisotropic effects.[10] Thus, it would appear that the upfield-shifted signals observed in this instance do not provide definitive evidence for π-type complexation.

Having at that point been unable to discern by NMR experiments the precise mode by which benzaldehyde was bound in complex **3′**, but with strong evidence supporting the formation of a (*R*)-BINAP·$(AgF)_2$*$(O{=}C(H)Ph)_n$ complex, we turned to DFT calculations to develop a better understanding of the structural features of **3′**. To this end, σ- and π-bound complexes of (*R*)-BINAP·$(AgF)_2$*$(O{=}C(H)Ph)_n$ having one or two benzaldehyde ligands were optimized in the gas phase at room temperature at the B3LYP/DGDZVP (density Gauss double-ζ with polarization functions basis set) level.[11] Interestingly, upon optimization of those geometries initiated from π-type complexes, it was immediately brought to our attention that they inevitably converged to σ-type complexes. Nevertheless, out of those conformers considered, minima **4**−**6** were found to be the lowest in energy (Figure 2). With respect to these conformers, present in **6** was a μ^2-σ-coordinated benzaldehyde, whereas the benzaldehyde in structures **4** and **5** was η^1-σ-coordinated.

The influence of temperature and solvent effects upon these complexes was then considered by reoptimizing these structures at 193, 212, and 249 K and room temperature with the IEFPCM (integral equation formalism polarizable continuum model) method to account for the solvent methanol generally employed in practice. These calculations indicated that aldehyde-bound complex **5** was the lowest energy structure among **4**−**6** (see Figure 2 and Supporting Information). However, we discerned from an analysis of the computed Mulliken charges of these three complexes that the carbonyl carbon of the bridged structure **6** was more electron-deficient then those of **4** and **5**, suggesting that allylation likely proceeds

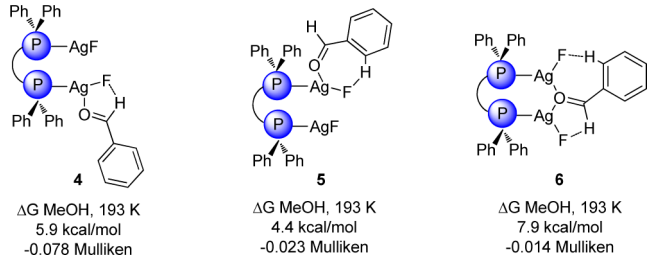

Figure 2. Global and competing minimal geometries, free energies of complexation (ΔG), condensed to carbonyl carbon Mulliken charge analysis for the catalytic complex calculated at the DFT B3LYP/DGDZVP level of theory.

through a less stable, albeit kinetically more reactive, intermediate such as **6** instead of the thermodynamically more stable minimum **5**.[12] Along these same lines, consistent with **6** being the major catalytic complex governing stereoinduction in this reaction, a visual inspection of these three species revealed that the *si*-face of the bound aldehyde in structures **4** and **5** was sterically unhindered and open to attack. Alternatively, if allylation ensued from **6**, the sense of stereoinduction would be consistent with the experimentally observed *re*-facial stereoselectivity because the *si*-face of the aldehyde is shielded by the catalyst.

However, at odds with the computed nonsymmetrical nature of **4**−**6** was our experimental observation of a single ^{31}P NMR shift at 10.6 ppm that implied the two phosphorus atoms of the catalyst-bound aldehyde adduct formed in this reaction were chemically shift equivalent. In view of this discrepancy and to clarify this point further, we once again turned to DFT calculations carried out within the framework of GIAO−DFT (B3LYP/DGDZVP) NMR theory to help elucidate the structure of (*R*)-BINAP·$(AgF)_2$*$(O{=}C(H)Ph)$ (**4**−**6**). From these calculations we concluded that the ^{31}P NMR resonances of structure **5** were downfield from those of the parent complex (*R*)-BINAP·$(AgF)_2$ (that is, catalyst **3**), whereas those of **4** and **6** were shifted upfield with respect to **3** (Table 2). Surprisingly, the difference in chemical shift between the two phosphorus atoms in **5** of 0.3 ppm was smaller than that of **4** and **6**. However, it should be noted that this minute difference between the computed ^{31}P chemical shifts would not be apparent from our experimental NMR results, even if it were the two phosphorus atoms would appear to be equivalent on the NMR time scale if there was rapid ligand exchange between the two silver atoms of **5**. Interestingly, the shift difference ($\Delta\delta$) in ^{31}P NMR between **3** and **5** was found to decrease with temperature, whereas the inverse trend was observed for **4** and **6** in relation to **3**. A small, upfield shift was observed in the calculated ^{1}H signal corresponding to the aldehydic hydrogen of **5**, but an inverse trend was observed for **4** and **6**. All of the carbonyl carbons of **4**−**6** were shifted downfield. The differences between the calculated and experimental magnitudes of $\Delta\delta$ ^{31}P NMR shifts are thought to arise from two sources: the intrinsic conformational dynamics of the (*R*)-BINAP·$(AgF)_2$*$(O{=}C(H)Ph)$ complex that, because of the demanding nature of these calculations, could not be accounted for *in silico* and the inadequate treatment of the long-range effects at the level of theory used.[13] The latter could also contribute to the inconsistencies between experimental and computed ^{1}H proton and ^{13}C carbon shifts because the inductive effect of the large aromatic system of the catalyst could have a significant impact on the magnetic susceptibilities

dx.doi.org/10.1021/jo400451u | J. Org. Chem. 2013, 78, 4440−4445

Table 2. Computed Relative Chemical Shifts from GIAO−DFT Calculations[a]

	249 K Δδ			212 K Δδ			193 K Δδ		
	$^{31}P^b$	$^{13}C^c$	$^{1}H^c$	$^{31}P^b$	$^{13}C^c$	$^{1}H^c$	$^{31}P^b$	$^{13}C^c$	$^{1}H^c$
4	−1.5	6.3	0.32	−1.5	6.3	0.32	−1.0	6.3	0.32
5	1.5	1.0	−0.25	1.5	1.0	−0.25	2.0	1.0	−0.25
6	−4.2	0.9	0.06	−4.2	0.9	0.06	−3.8	0.9	0.06

[a]Chemical shifts were computed for modeled structures **4**–**6** by GIAO−DFT at the B3LYP/DGDZVP level from the difference of isotropic shielding tensors from the reference structure by the following equation: $\Delta\delta = \sigma - \sigma_{ref}$. [b]The differences of ^{31}P shifts were found using structure **3** as a reference. [c]The differences of ^{13}C and ^{1}H shifts were found using the structure of benzaldehyde calculated at the same level of theory.

of neighboring nuclei. Moreover, the binding of a second benzaldehyde to either **4** or **5**, which would more readily allow for the generation of a symmetric complex, was associated with an additional cost of 7.1 or 5.0 kcal/mol at 193 K, respectively, and is therefore unlikely.

Privy to the above insight and in an attempt to gain a clearer mechanistic understanding of how complex **6** facilitated allylation, we monitored by NMR the subsequent effect of added allyltrimethoxysilane (allyl-Si(OMe)$_3$, 1.5 equiv) on the cooled (T = 234 K) methanol-d_4 solution of the catalyst (*R*)-BINAP/AgF (10:6, 0.1 equiv) and benzaldehyde (1 equiv). Readily apparent from the resulting ^{31}P NMR spectrum was that the signal assigned to **5** had markedly broadened, whereas that assigned to **3** had completely disappeared. In view of this dramatic change, the mixture was cooled further in an attempt to resolve the broad overlapping signals of **1** and **2**. This proved to be ineffective but nevertheless did lend further support to the ideas that a (*R*)-BINAP·(AgF)$_2$*(O═C(H)Ph)$_n$ complex such as **6** formed under the reaction conditions, and that this intermediate was a key mechanistic precursor to allylation.

To further expand upon this last idea, a subsequent in-depth ^{29}Si NMR analysis revealed that besides three major silicon species observed at −45.9 ppm (s), −77.3 ppm (s), and −84.9 ppm (m), one minor intermediate [−54.2 ppm (m)] was formed at −80 °C in the reaction mixture. After the mixture was warmed to −10 °C, the ^{29}Si signals assigned to the major and minor ^{29}Si adducts of this mixture observed at −45.9 and −54.2 ppm (m) disappeared, and the relative intensity of the −77.3 ppm signal to the −84.9 ppm signal increased (see Supporting Information). As for the identity of the silicon species observed at −45.9 and −77.3 ppm, it was determined by direct comparison with both an authentic sample prepared in-house and reported ^{29}Si NMR data that they corresponded to allyltrimethoxysilane (−45.9 ppm) and tetramethoxysilane (TMOS, −77.3 ppm).

Also in agreement with this assignment were $^{29}Si-^{1}H$ HSQC experiments that revealed the three signals corresponding to allylic and olefinic protons of the parent allyltrimethoxysilane were strongly coupled to the silicon signal at −45.9 ppm. Furthermore, all four of the observed silicon signals were found to be strongly coupled to protons in the same spectral region as those of the methoxysilane protons of the parent allylsilane reagent at ∼3 ppm. In addition, the ^{29}Si signals at −77.3 and −84.9 ppm were not coupled to any other protons. As for the minor silicon adduct, there was visible coupling to protons having significant overlap with the allylic and olefinic protons of the parent allylsilane. Although this made assignment of this signal difficult, allyltrialkoxysilanes are known to form activated silyl anions in the presence of halides;[14] however, their ^{29}Si chemical shifts normally occur between −110 and −130 ppm.[15] Consequently, we conjectured that this signal arises from the transient formation of an activated, hypervalent allyltrimethoxysilane derivative that is strongly deshielded in this reaction scenario.

From there we turned to GIAO−NMR DFT calculations to aid in the assignment of the −83.5 ppm signal. Fluorinated silanes were considered a likely candidate for the −84.5 ppm signal, and as such fluorotrimethoxysilane (Si(OMe)$_3$F) was thought to be a reasonable starting point.[16] The structure of Si(OMe)$_3$F was optimized at the (GIAO−DFT) B3LYP/6-311G+(2d,p)//B3LYP/DGDZVP level of theory.[17] The structures of allyl-Si(OMe)$_3$ and Si(OMe)$_4$ were also optimized in the same manner to corroborate our experimental results with our computational methodology. Notably, there was a strong correlation between our experimentally observed and calculated chemical shifts both in trend and in magnitude (Table 3). More specifically, the calculated shift for Si(OMe)$_3$F follows the same bias in relation to allyl-Si(OMe)$_3$ and Si(OMe)$_4$ observed for the experimentally assigned shifts.

Table 3. Computed ^{29}Si Chemical Shifts Using GIAO−DFT Calculations[a]

intermediate	DGDZVP (ppm)	6-311G+(2d,p) (ppm)	experiment (ppm)
allyl-Si(OMe)$_3$	−40.2	−56.0	−45.9
Si(OMe)$_4$	−58.3	−85.2	−77.3
Si(OMe)$_3$F	−66.8	−91.9	−84.9

[a]All ^{29}Si NMR chemical shifts were computed using GIAO−DFT at the B3LYP/DGDZVP and B3LYP/6-311G+(2d,p) levels on optimized structures at the corresponding level of theory. Shifts are relative to computed shifts of trimethylsilane at the corresponding level of theory.

Taking into consideration the above results and building upon related previously reported mechanistic work, we tentatively propose the mechanistic cycle outlined in Scheme 2. The cycle begins with coordination of a single benzaldehyde to **3** to generate a rapidly interconverting mixture of catalyst-bound complexes such as **4**, **5**, and **6**. Of these complexes, the two-metal center bifurcated mode of Ag binding present in **6** leads to greater activation of the carbonyl carbon of benzaldehyde, as indicated above by our Mulliken charge analysis, likely making **6** the predominant species by which carbon−carbon bond formation occurs. Another notable feature of **6**, as mentioned above, is the fact that the *si*-face of benzaldehyde is well-shielded by the aromatic system of the catalyst, whereas the *re*-face is sterically unhindered. Assuming that allylation takes place at the less sterically shielded *re*-face of benzaldehyde via a structural arrangement such as **6**, the reaction outcome would be consistent with the stereoselectivity of the Sakurai−Hosomi−Yamamoto allylation observed experimentally when using (*R*)-BINAP. From **6**, transallylation ensues to generate a rapidly interconverting assembly of highly

dx.doi.org/10.1021/jo400451u | J. Org. Chem. 2013, 78, 4440−4445

Scheme 2. Proposed Catalytic Cycle

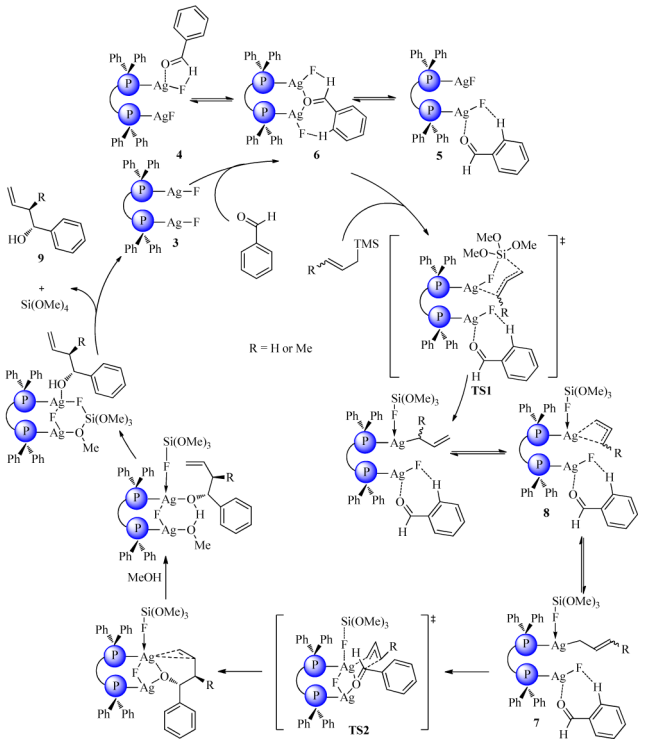

reactive η^1-allyl (**7**) and η^3-allyl (**8**) species, which, depending on their lifetimes, would allow for potential regiochemical scrambling under the reaction conditions. As such, allylation of benzaldehyde thereafter could foreseeably proceed from either **7** or **8**; however carbon−carbon bond formation would take place at the most substituted terminus of the allyl fragment, which is in accord with the regioselectivity findings involving crotylsilanes reported by Yamamoto et al.[18] The closed chairlike transition state (**TS2**) would help account for the reported strong *anti* diastereoselectivity that occurs independently of the configuration of the starting crotyl- and allylsilanes in these reactions.[19] Alternatively, one could invoke formation of the Ag−allyl species prior to benzaldehyde binding. In either case, the following allylation would proceed with the same regio-, enantio-, and diastereoselectivities. Further modeling of transition state assemblies for the transallylation and allylation processes is warranted to determine which of these pathways are favored. To complete the catalytic cycle, we propose the coordination of methanol to a silver center that catalyzes proton transfer to generate the homoallylic alcohol **9** and sets up for a ligand exchange between fluorotrimethoxysilane and the silver−methoxy complex to regenerate the catalyst and form TMOS.[20] The exact mechanism of this proton transfer is not well understood, and we cannot determine if methanol is involved directly in the allylation transition state or if this occurs in a stepwise manner after allylation.

CONCLUSION

The results of our research suggest that three distinct coordination complexes are formed in a mixture of AgF and (*R*)-BINAP, only one of which forms a catalytic complex with benzaldehyde. Computational results suggest that the lowest energy conformer of this complex corresponds to an η^1-bound complex which by rotation can lead to a highly activated μ^2-bound complex. We have detected the formation of two silicon species from allyltrimethoxysilane both in the presence and in the absence of benzaldehyde. Comparison to authentic samples and GIAO−DFT calculated shifts suggest that these are TMOS and fluorotrimethoxysilane. The results of this study provide valuable insight into the catalytic species and their corresponding intermediary ground state complexes, laying the groundwork for computational modeling of allylation transition states and the eventual complete elucidation of this mechanism.

EXPERIMENTAL SECTION

NMR experiments were conducted on an instrument operating at 600 MHz. All reagents were used directly from the bottle without further purification.

Representative NMR Methodology. To a dry NMR tube was added 1.5 mL of a solution of (*R*)-BINAP (3.8 mg, 0.0061 mmol) and AgF (1.5 mg, 0.012 mmol) in methanol-d_4. The corresponding ^{31}P, ^{13}C, ^{1}H, and ^{13}C−^{1}H HSQC NMR spectra were obtained at the reported temperatures.

Benzaldehyde (13 μL, 0.12 mmol) was then added; the sample was shaken, and the corresponding ^{31}P, ^{13}C, ^{1}H, and ^{13}C−^{1}H HSQC NMR spectra were obtained at the reported temperatures.

To the above mixture was added allyltrimethoxysilane (30 μL, 0.18 mmol); the sample was shaken, and the corresponding ^{31}P, ^{13}C, ^{1}H, ^{29}Si, ^{13}C−^{1}H HSQC, and ^{29}Si−^{1}H HSQC spectra were obtained at the reported temperatures.

ASSOCIATED CONTENT

Supporting Information

Thermochemical and structural data for calculations in the gas phase at room temperature for the catalyst−benzaldehyde complex; thermochemical, GIAO−DFT, and structural data for calculations using the IEFPCM method for methanol at 193, 212, and 249 K for the catalyst−benzaldehyde complex; thermochemical, GIAO−DFT, and structural data for silicon intermediates; and NMR spectra. This material is available free of charge via the Internet at http://pubs.acs.org.

AUTHOR INFORMATION

Corresponding Author

*tdudding@brocku.ca

Notes

The authors declare no competing financial interest.

ACKNOWLEDGMENTS

The authors thank Compute Canada for use of SHARC Net. We are grateful to the Natural Sciences and Engineering Research Council of Canada (NSERC) for funding of this research.

REFERENCES

(1) (a) Hosomi, A.; Sakurai, H. *Tetrahedron Lett.* **1976**, *17*, 1295. (b) Hosomi, A.; Sakurai, H. *J. Am. Chem. Soc.* **1977**, *99*, 1673.

(2) (a) Denmark, S. E.; Almstead, N. G. In *Modern Carbonyl Chemistry*; Otera, J., Ed.; Wiley-VCH: Weinheim, Germany, 2000; p 299. (b) Chemler, S. R.; Roush, W. R. In *Modern Carbonyl Chemistry*; Otera, J., Ed.; Wiley-VCH: Weinheim, Germany, 2000; pp 403.

(3) (a) Yanagisawa, A.; Kageyama, H.; Nakatsuka, Y.; Asakawa, K.; Matsumoto, Y.; Yamamoto, H. *Angew. Chem.* **1999**, *111*, 3916; *Angew. Chem., Int. Ed.* **1999**, *38*, 3701. (b) Yamamoto, H.; Wadamoto, M. *Chem.−Asian J.* **2007**, *2*, 692. For a recent review on catalytic enantioselective allylation, see: (c) Yus, M.; Gonzalez-Gomez, J. C.; Foubelo, F. *Chem. Rev.* **2011**, *111*, 7774. For recent papers discussing catalytic enantioselective carbonyl allylation reactions, see: (d) Haddad, T. D.; Hirayama, L. C.; Singaram, B. *J. Org. Chem.* **2010**, *75*, 642.

(e) Hrdina, R.; Valterova, I.; Hodacova, J.; Cisarova, I.; Kotora. *Adv. Synth. Catal.* **2007**, *349*, 822.
(4) Ohkouchi, M.; Masui, D.; Yamaguchi, M.; Yamagishi, T. *J. Mol. Catal. A: Chem.* **2001**, *170*, 1.
(5) (a) Wadamoto, M.; Yamamoto, H. *J. Am. Chem. Soc.* **2005**, *127*, 14556. (b) For a detailed isolation and characterization of an AgOTf/BINAP catalyst that afforded high levels of enantioselectivity in a nitrosoaldol addition of allyltin reagents, see: Momiyama, M.; Yamamoto, H. *J. Am. Chem. Soc.* **2004**, *126*, 5360. By scanning metal:ligand ratios the authors were able to select for the exclusive formation of one of three silver−BINAP complexes, allowing for isolation and subsequent structural characterization of these complexes by X-ray diffraction. The primary catalytic species that was found to be responsible for the high levels of enantioselectivity observed in this nitrosoaldol addition was structurally analogous to complex **3** proposed in our study.
(6) (a) Denmark, S. E.; Fu, J. *Chem. Rev.* **2003**, *103*, 2763. (b) Denmark, S. E.; Beutner, G. L. *Angew. Chem., Int. Ed.* **2008**, *47*, 1560.
(7) (a) Muetterties, E. L.; Alegranti, C. W. *J. Am. Chem. Soc.* **1972**, *84*, 6386. (b) Goel, R. G.; Pilon, P. *Inorg. Chem.* **1978**, *17*, 2876.
(8) (a) Gutowsky, H. S.; Holme, C. H. *J. Chem. Phys.* **1956**, *25*, 1228. (b) Evans, M. G.; Polanyi, M. *Trans. Faraday Soc.* **1935**, *31*, 875.
(9) (a) Gladysz, J. A.; Boone, B. J. *Angew. Chem., Int. Ed.* **1997**, *36*, 550. (b) Reetz, M. T.; Hüllmann, M.; Massa, W.; Berger, S.; Radmacher, P.; Heymanns, P. *J. Am. Chem. Soc.* **1986**, *108*, 2405. (c) Denmark, S. E.; Almstead, N. G. *J. Am. Chem. Soc.* **1993**, *115*, 3133. (d) Peterson, E.; Khalimon, A. Y.; Simionescu, R.; Kuzmina, L. G.; Howard, J. A. K.; Nikonov, G. I. *J. Am. Chem. Soc.* **2009**, *131*, 908. (e) Fernández, J. M.; Emerson, K.; Larsen, R. H.; Gladysz, J. A. *J. Am. Chem. Soc.* **1986**, *108*, 8268.
(10) Pregosin, P. S.; Ruegger, H.; Salzmann, R.; Albinati, A.; Lianza, F.; Kunz, R. W. *Organometallics* **1994**, *13*, 83.
(11) The DGDZVP basis set has been shown to provide accurate vibrational frequencies for silver and other transition-metal complexes, see: (a) Godbout, N.; Salahub, D. R.; Andzelm, J.; Wimmer, E. *Can. J. Chem.* **1992**, *72*, 60. (b) Sosa, C.; Andzelm, J.; Elkin, B. C.; Wimmer, E.; Dobbs, K. D.; Dixon, D. A. *J. Phys. Chem.* **1992**, *96*, 6630.
(12) Our previous studies of modeling transition states of analogous indium catalysts suggested a bridged coordination mode of the oxygen in the transition state. See: Mirabdolbaghi, R.; Dudding, T. *Org. Lett.* **2012**, *14*, 3748.
(13) Although the use of perturbation theory (MP2) was seen as a possible resolution to this problem as it accounts for long range interactions more accurately, see: Gauss, J. *Phys. Chem. Chem. Phys.* **1995**, *99*, 1001. Due to the associated computational cost of modeling a system of this size, and given that the trends in computed phosphorus shifts were consistent with experiment, the pursuit of higher level calculations was deemed unnecessary.
(14) (a) Sato, K.; Kira, M.; Sakurai, H. *J. Am. Chem. Soc.* **1989**, *111*, 6429. (b) Cerveau, G.; Chuit, C.; Corriu, R. J. P.; Reye, C. *J. Organomet. Chem.* **1987**, *328*, C17. (c) Hosomi, A.; Kohra, S.; Tominaga, Y. *J. Chem. Soc., Chem. Commun.* **1987**, 1517.
(15) Holmes, R. R. *Chem. Rev.* **1996**, *96*, 927.
(16) Wadamoto, M.; Ozasa, N.; Yanagisawa, A.; Yamamoto, H. *J. Org. Chem.* **2003**, *68*, 5593.
(17) The standard methodology established by Cheeseman et al. indicated that the most accurate chemical shifts can be obtained at the B3LYP/6-311G+(2d,p) level for DFT calculations. See: Cheeseman, J. R.; Trucks, G. W.; Keith, T. A.; Frisch, M. J. *J. Chem. Phys.* **1996**, *104*, 5497. The ^{31}P shifts could not be calculated with this basis set due to the presence of silver in the investigated structures.
(18) Wadamoto, M.; Naodovic, M.; Yamamoto, H. *Eur. J. Org. Chem.* **2009**, 5132.
(19) Aoyama, N.; Hamada, T.; Manabe, K.; Kobayashi, S. *J. Org. Chem.* **2003**, *68*, 7329.
(20) It is understood that the presence of methanol leads to a notable increase in the overall yield of this reaction. See: Wadamoto, M.; Yamamoto, H. *J. Am. Chem. Soc.* **2005**, *127*, 14556. The significant impact of methanol and the eventual fate of silicon as TMOS lead us to believe that methanol is involved in the slow regeneration of the catalyst and formation of TMOS from fluorotrimethoxysilane.